# 3.3 Strongly Correlated Quantum Systems

# Development and application of quantum many-body solver

Masatoshi IMADA
*Physica Division, Department of Engineering and Applied Sciences, Sophia University, 7-1 Kioi-cho, Chiyoda-ku Tokyo, 102-8554*

Accurate description of ground-state wave functions of fermionic many-body systems and applications of the method to strongly correlated electron systems are the target of this project. Neural network combined with the pair-product (Pfaffian) wave function is a promising way for this purpose. Along this line, restricted Boltzmann machine has established an accurate way to approximate ground states of quantum spin systems [1] as well as itinerant fermion systems [2].

The Boltzmann machine introduces hidden variables that are described by classical degrees of freedom. In this project, we are exploring the way mapping of interacting lattice fermions such as the Hubbard model to noninteracting multi-component fermion models in the ground states, from which we have proposed a quantum machine learning algorithm called Fermi machine aiming at an efficient quantum many-body solver [3]. Fermion systems are introduced as the hidden part coupled to the physical system, instead of the classical one such as the Ising spins in the previous Boltzmann machine. This algorithm has been inspired by recent success of fractionalized fermions to describe experimental results of the cuprate superconductors [4–9].

In contrast to the conventional variational Monte Carlo method [10], the present Fermi machine can easily treat the entanglement with the hidden fermion degrees of freedom hybridizing with the physical (visible) fermions, thus allows the formation of the gap structure in the spectra without spontaneous symmetry breaking, generating zeros of the Green's functions as well as poles, which is characteristic of the genuine Mott insulator. Exploration of efficient algorithms for larger systems is under way.

In the application part, the algorithm with neural network combined with the pair-product wave function was recently successfully applied to cuprate superconductors and reproduced the universality and materials dependence [11, 12].

The project was financially supported by MEXT KAKENHI, Transformative Research Area (Grant No. JP22H05111 and No. JP22H05114). and also supported by MEXT under the grant number JPMXP1020230411.

## References

[1] G. Carleo and M. Troyer, Science **355**, 602 (2017).

[2] Y. Nomura, *et al.*, Phys. Rev. B **96**, 205152 (2017).

[3] M. Imada. J. Phys. Soc. Jpn. **93**, 104002 (2024).

[4] S. Sakai, M. Civelli, and M. Imada, Phys. Rev. Lett. **116**, 057003 (2016).

[5] Y. Yamaji *et al.*, Phys. Rev. Research **116**, 057003 (2021).

[6] M. Imada: J. Phys. Soc. Jpn. **90**, 111009 (2021).

[7] A. Singh *et al*, Nat. Commun. **13**,7906 (2022).

[8] M. Horio *et al.* PNAS **122**, e2406624122 (2025).

[9] S. Sakai *et al.*, Phys. Rev. X **16** 011018 (2026).

[10] T. Misawa *et al.* Comput. Phys. Commun. **235**, 447 (2019).

[11] M. Schmid *et al.*, Phys. Rev. X **13**, 041036 (2023) .

[12] R. Kaneko snd M. Imada, unpublished.

# Exotic superconductivity in the doped Kitaev spin liquid

Takahiro MISAWA
*Institute for Solid State Physics, University of Tokyo*
*Kashiwa-no-ha, Kashiwa, Chiba 277-8581*

The Kitaev model on the honeycomb lattice is a rare exactly solvable spin model whose ground state is a quantum spin liquid (QSL) [1]. It has been proposed that Kitaev interactions dominate in Mott insulators with strong spin-orbit coupling, such as $\alpha$-$RuCl_3$ and iridates [2, 3]. It is expected that carrier doping of such a QSL is a promising route to exotic superconductivity (SC). Mean-field studies of the doped Kitaev model predicted triplet $p$-wave and singlet $d+id$ pairing [4, 5, 6], but controlled results beyond mean-field theory have been scarce. In this project we studied the hole-doped $t$-$J$-type Kitaev model by the many-variable variational Monte Carlo (mVMC) method, focusing on the ferromagnetic (FM) Kitaev interaction.

We consider the Hamiltonian

$$\mathcal{H} = -t \sum_{\langle i,j\rangle,\sigma} \left( c^{\dagger}_{i\sigma} c_{j\sigma} + \text{H.c.} \right) + \sum_{\langle i,j\rangle_{\alpha}} K_{\alpha}\, S^{\alpha}_{i} S^{\alpha}_{j}$$

on the honeycomb lattice, with isotropic coupling $K_x = K_y = K_z \equiv K$ (FM corresponds to $K < 0$, and we set $K/t = -1$) and hole concentration $\delta = 1 - N_e/N_s$. We use a Gutzwiller-projected pair-product (Pfaffian) wave function with a density-density Jastrow factor, optimized by stochastic reconfiguration. Double occupancy is completely excluded by the Gutzwiller projection. In the actual calculations, we use the open-source software mVMC [7]. This wave function exactly reproduces the Kitaev-QSL ground state at half filling, giving a controlled starting point for doping. The calculations were mainly performed on System B ("ohtaka") of the Supercomputer Center, ISSP.

For the FM Kitaev interaction, we find that the triplet $p$-wave pairing correlations show plateaus at long distances, while singlet correlations remain negligible. The long-range-averaged $p$-wave correlation forms a dome as a function of hole doping. The correlation peaks around $\delta \simeq 0.2$ and shows essentially no size dependence for $\delta \lesssim 0.2$. This signals robust triplet $p$-wave superconductivity. For $\delta \gtrsim 0.2$, a saturated ferromagnetic state appears, where the magnetization reaches the fully polarized value $(1-\delta)/2$ and the $p$-wave correlations are sharply suppressed. This shows that the magnetic background generated by doping controls the pairing.

In summary, using the mVMC method with a pair-product wave function that exactly reproduces the Kitaev QSL at half filling, we have shown that the hole-doped FM Kitaev model hosts robust triplet $p$-wave superconductivity in a finite doping window, which is suppressed by full ferromagnetic polarization. Investigating the effects of additional interactions, such as Heisenberg and off-diagonal $\Gamma$ terms, is left for future work.

## References

[1] A. Kitaev, Ann. Phys. **321**, 2 (2006).

[2] G. Jackeli and G. Khaliullin, Phys. Rev. Lett. **102**, 017205 (2009).

[3] Y. Motome and J. Nasu, J. Phys. Soc. Jpn. **89**, 012002 (2020).

[4] Y.-Z. You, I. Kimchi, and A. Vishwanath, Phys. Rev. B **86**, 085145 (2012).

[5] T. Hyart, A. R. Wright, G. Khaliullin, and B. Rosenow, Phys. Rev. B **85**, 140510(R) (2012).

[6] S. Okamoto, Phys. Rev. B **87**, 064508 (2013).

[7] T. Misawa *et al.*, Comput. Phys. Commun. **235**, 447 (2019).

# Strong-coupling superconductivity in bilayer Hubbard model

Yusuke NOMURA

*Institute for Materials Research (IMR), Tohoku University,*

*2-1-1 Katahira, Aoba-ku, Sendai 980-8577*

The quest to understand high-transition temperature ($T_c$) superconductivity (SC) remains a central issue in condensed matter physics. In this context, the recent discovery of high-$T_c$ SC in $La_3Ni_2O_7$ has generated significant interest [1].

As a canonical model hosting high-$T_c$ SC and as an effective model for $La_3Ni_2O_7$, we investigate the bilayer Hubbard model on a square lattice [2] using state-of-the-art cluster dynamical mean-field theory. Unlike the *d*-wave SC observed in doped Mott insulators such as cuprates, the bilayer model exhibits *s*±-wave SC emerging from a correlated band insulator, where dynamical band repulsion drives the insulating behavior [3]. We uncover kinetic-energy-driven SC in a small doping region and its crossover to conventional potential-energy-driven SC. Above $T_c$, we observe an unusual metallic state with a striking momentum-space dichotomy in the kinetic-energy-driven regime: one Fermi pocket develops a pseudogap while the other becomes nearly incipient.

Despite differences in pairing symmetry and parent insulating states, we identify the strong momentum-space dichotomy as a remarkable commonality between the *d*-wave SC (antinodal vs. nodal regions) and the *s*±-wave SC (electron vs. hole pockets). The dichotomy in the bilayer system arises from self-energy differences between bonding and antibonding orbitals, further linking it to orbital-selective physics in iron-based superconductors.

Using a novel method for estimating the coherence length in strongly correlated SC [4], we reveal that the coherence length of the *s*±-wave SC is only a few lattice constants, corresponding to ~1 nm in $La_3Ni_2O_7$, which accounts for the exceptionally high critical field (~100 T) observed experimentally. This localized pairing may be driven by an effective pair-hopping term between bonding and antibonding orbitals, analogous to localized Cooper pairing in fullerides, in which the intramolecular pair-hopping term plays a crucial role [5].

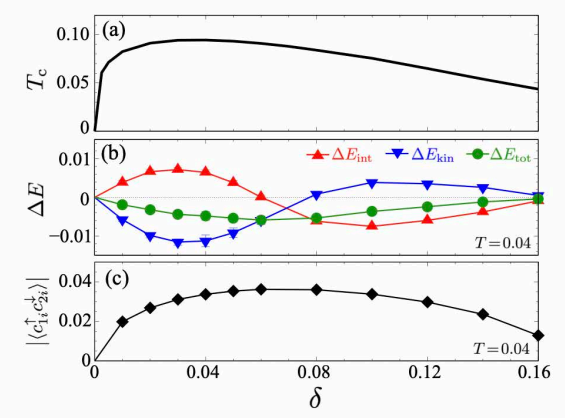


Fig. 1: Doping dependence of (a) $T_c$, (b) energy difference between SC and normal states at $T$ = 0.04, and (c) the SC order parameter at $T$=0.04 for the bilayer Hubbard model. The energy unit is set by the intralayer hopping. The interlayer hopping $t_\perp$ and Hubbard $U$ are set to $t_\perp$=2 and $U$=8, respectively.

## References

[1] H. Sun *et al*., Nature **621**, 493 (2023).

[2] Y. Nomura, M. Kitatani, S. Sakai, and R. Arita, Phys. Rev. B **112**, L020504 (2025)

[3] S. S. Kancharla and S. Okamoto, Phys. Rev. B **75**, 193103 (2007).

[4] N. Witt *et al*., npj Quantum Materials **9**, 100 (2024).

[5] Y. Nomura *et al.*, J. Phys.: Condens. Matter **28**, 153001 (2016).

# Multilayer effects on the coexistence of antiferromagnetism and superconductivity in cuprate superconductors: a variational Monte Carlo study

Ryui KANEKO
*Physics Division, Sophia University*
*Chiyoda, Tokyo 102-8554, Japan*

Clarifying the materials dependence of $T_c$ in cuprate superconductors would provide important clues for the search for materials with even higher $T_c$. Although the superconducting transition temperature $T_c$ depends strongly on the number of layers, to date, many first-principles studies of cuprate superconductors have focused on compounds with one or two layers. In contrast, the highest $T_c$ among cuprates is found in the trilayer compound $HgBa_2Ca_2Cu_3O_8$ (Hg1223), which exhibits $T_c \sim 138\,\mathrm{K}$ at ambient pressure and even higher $T_c \sim 164\,\mathrm{K}$ under pressure [1, 2].

In this study, we examined the possibility of the coexistence of antiferromagnetism and superconductivity by searching for the ground states of multilayer systems. In multilayer cuprate superconductors, it is often the case that superconductivity is realized in the outermost layers, while superconductivity and antiferromagnetism coexist in the inner layers. We used the three-layer Hg1223 system as a typical example and examined its ground state. We prepared an initial state with the outer layers being superconducting and the inner layers exhibiting the coexistence of superconductivity and antiferromagnetism. We investigated whether such a solution can be stably obtained after optimization over a wide range of doping concentrations.

Effective Hamiltonians for the multilayer system Hg1223, which exhibits the highest $T_c$ among cuprates, were obtained by first-principles calculations at ambient pressure (0 GPa) and under pressure (30 GPa and 60 GPa) [3]. These effective Hamiltonians are given by

$$H = \sum_{i,j,\sigma} t_{ij} c^{\dagger}_{i\sigma} c_{j\sigma} + \sum_{i} U_i n_{i\uparrow} n_{i\downarrow} + \frac{1}{2} \sum_{i \neq j} V_{ij} n_i n_j. \quad (1)$$

Here, for each pressure, the onsite Coulomb repulsion $U_i$ takes layer-dependent values, while the hopping $t_{ij}$ and the further neighbor Coulomb repulsion $V_{ij}$ for intralayers and interlayers are taken up to long-range values satisfying $|\mathbf{r}_i - \mathbf{r}_j| \leq 3\sqrt{2}$. We take the lattice constant as the length unit. For this effective Hamiltonian of Hg1223, we computed the ground state at an average doping concentration of approximately 10% using the many-variable variational Monte Carlo method [4], which enables large-scale parallel computation with MPI and OpenMP. Using a variational wave function constructed from a generalized pairing wave function supplemented by Gutzwiller–Jastrow correlation factors and combined with restricted Boltzmann machine correlation factors, we examined the $d$-wave superconducting state, as well as that coexisting with antiferromagnetism, as a candidate for the ground state.

By controlling the difference in chemical potential between the outer and inner layers so as to approach the parameter region consis-

tent with experiment, we found a ground-state candidate in which superconductivity is realized in both the outer and inner layers, and another ground-state candidate in which superconductivity is realized in the outer layers, whereas antiferromagnetic and superconducting orders coexist in the inner layer. Since the energies of these two states are highly competing, we further applied the Lanczos procedure and performed variance extrapolation to determine the ground state. As a result, we found a parameter region in which the ground state is a superconducting state in the outer layers and a coexistence of superconductivity and antiferromagnetism in the inner layer. The coexistence of antiferromagnetic and superconducting orders in multilayer cuprates is in agreement with experimental observations [5–7].

These results suggest that the layer-selective coexistence of antiferromagnetic and superconducting orders is not merely a competing instability but can be an essential ingredient of the ground state in multilayer cuprates. Therefore, the present study provides a microscopic perspective on the strong layer dependence of $T_c$ and highlights the importance of interlayer charge imbalance as a key parameter for enhancing superconductivity. Extending this analysis to other multilayer cuprates and systematically examining the pressure- and layer-number-dependent properties will be an important step toward establishing a materials-design principle for realizing even higher $T_c$.

## References

[1] L. Gao, Y. Y. Xue, F. Chen, Q. Xiong, R. L. Meng, D. Ramirez, C. W. Chu, J. H. Eggert and H. K. Mao, Phys. Rev. B **50**, 4260(R) (1994).

[2] A. Yamamoto, N. Takeshita, C. Terakura, and Y. Tokura, Nat. Commun. **6**, 8990 (2015).

[3] J.-B. Morée, Y. Yamaji, and M. Imada, Phys. Rev. Res. **6**, 023163 (2024).

[4] T. Misawa, S. Morita, K. Yoshimi, M. Kawamura, Y. Motoyama, K. Ido, T. Ohgoe, M. Imada, T. Kato, Comp. Phys. Commun., **235**, 447 (2019).

[5] H. Mukuda, S. Shimizu, A. Iyo, and Y. Kitaoka, J. Phys. Soc. Jpn. **81**, 011008 (2012).

[6] K. Kurokawa, S. Isono, Y. Kohama, S. Kunisada, S. Sakai, R. Sekine, M. Okubo, M. D. Watson, T. K. Kim, C. Cacho, S. Shin, T. Tohyama, K. Tokiwa, and T. Kondo, Nat. Commun. **14**, 4064 (2023).

[7] S.-i. Ideta, S. Adachi, T. Noji, S. Yamaguchi, N. Sasaki, S. Ishida, S.-i. Uchida, T. Fujii, T. Watanabe, W. O. Wang, B. Moritz, T. P. Devereaux, M. Arita, C.-Y. Mou, T. Yoshida, K. Tanaka, T.- K. Lee, and A. Fujimori, Nat. Commun. **16**, 9470 (2025).

# Topological superconductivity in quantum Hall superconductor hybrids

Koji Kudo

*Department of Physics,*

*Kyushu University, Fukuoka 819-0395, Japan*

Creation and manipulation of Abelian and non-Abelian anyons --- emergent particles that are neither bosons nor fermions --- is one of the central goals of modern condensed matter physics. We have studied hybrid systems of quantum Hall states and superconductors as a platform of topological phases hosting anyons.

We discovered a new state, which we call “repulsive-interaction-induced topological superconductivity” [1]. This state emerges in a hybrid system where an interacting electron system at the Landau level filling factor $\nu=1/2$ is proximity-coupled to a type-II *s*-wave superconductor. While the composite Fermi liquid state is realized in the absence of the superconducting proximity effect, we demonstrated that a distinct phase appears upon introducing a finite pairing potential. This state exhibits odd fermion parity, suggesting topological superconductivity. Furthermore, this state disappears as the repulsive interaction is turned off, highlighting its many-body nature. We employed exact diagonalization using the Lanczos algorithm, with a parallel implementation across multiple compute nodes.

As another platform for topological superconductivity, we considered a kagome magnet proximity-coupled to Rashba superconductor. We demonstrated the emergence of scalar-spin-chirality-induced topological superconductivity in this system. We characterized this topological phase by numerically calculating the chiral central charge [2].

We also discussed fractional phases realized in kagome magnets. The exact diagonalization study demonstrated the emergence of the fractional Chern insulating state over a wide region of parameter space [3].

## References

[1] K. Kudo, R. Nakai, H. Isobe, J. K. Jain, and K. Nomura, arXiv:2510.04700.

[2] K. Kudo, R. Nakai, H. Isobe, and K. Nomura, arXiv:2602.07383.

[3] S. Tsutsumi, K. Kudo, and. K. Nomura, in preparation.

# Theoretical study of strongly correlated quantum properties by mathematical information science

Yukitoshi MOTOME

*Department of Applied Physics,*

*The University of Tokyo, Bunkyo, Tokyo 113-8656*

We have conducted theoretical investigations of a wide range of strongly correlated electron systems using advanced numerical approaches, including first-principles calculations, quantum many-body methods, and machine-learning techniques (project numbers: 2025-Ca-0095 and 2025-Cb-0008). We have also established several collaborative efforts with experimental groups. During the last fiscal year, we achieved substantial progress in the following areas.

(i) *Topological spin textures*: By examining the interactions between magnetic hopfions—closed rings formed by twisted skyrmion tubes—we proposed a stable periodic array of magnetic hopfions [1]. Furthermore, we demonstrated that spin–orbit torque induced by a spin current can drive the splitting dynamics of a hopfion with a higher Hopf number into multiple hopfions with lower Hopf numbers [2,3]. In addition, we introduced an efficient method for hopfion creation by applying an electric current to magnetic torons, which consist of a hedgehog–antihedgehog pair connected by a skyrmion tube [4].

(ii) *Spin-orbital coupled physics*: In collaboration with experimental groups, we elucidated that antiferromagnetic olivine compounds exhibit anomalous nonlinear magnetoelectric effects arising from electric-field-induced magnetic toroidal moments [5]. We also worked closely with experimental collaborators to determine the high-magnetic-field phase diagrams of $Pb(TiO)Cu_4(PO_4)_4$, a material characterized by active magnetic quadrupole degrees of freedom [6]. In addition, we conducted collaborative research leading to the discovery of a *p*-wave magnetic material [7] and to the clarification of its exotic physical properties [8].

(iii) *Quantum spin liquids*: We revealed the existence of topological Majorana flat bands in the Kitaev model defined on a periodically depleted honeycomb lattice [9]. We also investigated the competition among different types of quantum-disordered states, including the interplay between quantum spin liquid, spin-glass, and quantum paramagnetic phases in an extended Sachdev–Ye–Kitaev model [10], as well as the competition between the Kitaev spin liquid and the Affleck–Kennedy–Lieb–Tasaki valence-bond-solid state in an $S$=3/2 spin model on the honeycomb lattice

[11]. In addition, we carried out a series of studies on higher-spin spin-ice models on the pyrochlore lattice [12–14]. We also authored a review paper on α-$RuCl_3$, a prime candidate material for realizing Kitaev spin liquids [15]. Furthermore, we carried out collaborative research on a heterostructure system, which represents a promising platform for realizing a Kitaev spin-liquid state [16].

(iii) *Machine learning related*: In the context of quantum reservoir computing, which employs quantum many-body systems as reservoirs, we demonstrated that computational performance is maximized at the edge of chaos between ordered and chaotic regimes, thereby establishing a fundamental design principle for quantum reservoir computing [17]. We also published two papers proposing a newly developed framework termed *quantum reservoir probing*, which serves as an inverse approach to quantum reservoir computing and enables the extraction of physical information from complex quantum systems [18,19].

## References

[1] S. Kasai, K. Shimizu, S. Okumura, Y. Kato, and Y. Motome, Phys. Rev. B **112**, 184424 (2025).

[2] S. Kasai, S. Okumura, and Y. Motome, preprint (arXiv:2511.23027), to appear in APS Open Science.

[3] S. Kasai, S. Okumura, and Y. Motome, preprint (arXiv:2511.23045), to appear in Phys. Rev. B (Editors' Suggestion).

[4] A. Kajihara, S. Okumura, and Y. Motome, preprint (arXiv:2602.05332), to appear in Phys. Rev. B.

[5] Y. Kato, T. Hayashida, K. Matsumoto, T. Kimura, and Y. Motome, Phys. Rev. B. **113**, 094411 (2026).

[6] Y. Ihara *et al.*, Phys. Rev. B **112**, 094405 (2025).

[7] R. Yamada *et al.*, Nature **646**, 837 (2025).

[8] S. Okumura, M. M. Moritz, and Y. Motome, preprint (arXiv:2512.14071).

[9] K. Fukui and Y. Motome, Phys. Rev. B **112**, 14411 (2025).

[10] S. Wadashima and Y. Motome, Phys. Rev. B **112**, 214204 (2025).

[11] S. Ikegami, K. Fukui, R. Pohle, and Y. Motome, preprint (arXiv:2512.06322).

[12] S. Watanabe, Y. Motome, and H. Watanabe, preprint (arXiv:2603.03852).

[13] S. Watanabe, Y. Motome, and H. Watanabe, preprint (arXiv:2603.19620).

[14] S. Watanabe, Y. Motome, and H. Watanabe, preprint (arXiv:2604.04346).

[15] C. Ojeda-Aristizabal *et al.*, preprint (arXiv:2511.13838).

[16] M. Negishi *et al.*, Phys. Rev. Materials **9**, 086202 (2025).

[17] K. Kobayashi and Y. Motome, Phys. Rev. Lett. **136**, 040602 (2026).

[18] K. Kobayashi and Y. Motome, Nat. Commun. **16**, 3871 (2025).

[19] K. Kobayashi and Y. Motome, SciPost Phys. **18**, 198 (2025).

# Multipolar fluctuations in $CeRh_2As_2$ studied by DFT+DMFT method

Junya OTSUKI
*Research Institute for Interdisciplinary Science, Okayama University, Okayama 700-8530*

$CeRh_2As_2$ is a heavy-fermion superconductor that exhibits a nonsuperconducting transition at $T_0 \simeq 0.5$ K above $T_{SC}$ [1]. Its temperature-magnetic field ($T$–$H$) phase diagram is strongly anisotropic, with $T_0$ suppressed for $H \parallel c$ but enhanced for $H \perp c$. The order parameter of this phase has remained controversial between magnetic and quadrupolar scenarios. We apply first-principles approaches taking strong correlations into account to address possible order parameters in $CeRh_2As_2$.

We use density functional theory combined with dynamical mean-field theory (DFT+DMFT), implemented with the open-source software `DCore` [2]. We first derive the low-energy tight-binding model from fully relativistic DFT bands, and then incorporate local Coulomb correlations on Ce $4f$ orbitals within DMFT. We compute the momentum-dependent multipolar susceptibilities using the strong-coupling-limit (SCL) expression for the Bethe-Salpeter equation [3], implemented as `ChiQ` [4]. Both `DCore` and `ChiQ` have been developed with support from the Project for Advancement of Software Usability in Materials Science (PASUMS) [5]. We used the FAT node of System B to handle a sufficiently large system size and obtain reliable $\boldsymbol{q}$ dependence of the susceptibilities.

The calculated momentum-dependent susceptibilities show that the leading fluctuation is the magnetic dipole $M_z$ at $\boldsymbol{q} = (1/2, 1/2, 0)$, corresponding to a two-dimensional checkerboard configuration. The hybridization between the CEF ground-state and first-excited doublets further generates sizable magnetic octupole and electric quadrupole fluctuations. In particular, the fluctuations of $\{Q_{yz}, Q_{zx}\}$-type quadrupoles enhance fluctuations of the magnetic dipole $M_z$ under an in-plane magnetic field, leading to a $T$–$H$ phase diagram consistent with experiments. We thus proposed an antiferromagnetic $M_z$ order at $\boldsymbol{q} = (1/2, 1/2, 0)$ as the order parameter below $T_0$ in $CeRh_2As_2$ [6].

## References

[1] S. Khim *et al.*, Phys. Rev. Lett. **132**, 076504 (2024).

[2] H. Shinaoka, J. Otsuki, M. Kawamura, N. Takemori, and K. Yoshimi, SciPost Phys. **10**, 117 (2021).

[3] J. Otsuki, K. Yoshimi, H. Shinaoka, and Y. Nomura, Phys. Rev. B **99**, 165134 (2019).

[4] `https://github.com/issp-center-dev/ChiQ`.

[5] K. Yoshimi, Y. Motoyama, T. Aoyama, M. Kawamura, and N. Kawashima, Sci. Technol. Adv. Mater.: Methods **5**, 2564055 (2025).

[6] K. Numa, E. Matsuda, A. Kirikoshi, and J. Otsuki, Phys. Rev. B **113**, 115141 (2026).

# Dissipation-induced exotic superfluid phase in non-Hermitian Hubbard model

Akihisa Koga
*Department of Physics, Institute of Science Tokyo*
*Meguro, Tokyo 152-8551*

Open quantum systems have attracted significant interest due to their ability to exhibit novel phenomena absent in equilibrium settings. Recent advances in ultracold atom experiments have enabled the realization of dissipative many-body effects. In this context, non-Hermitian (NH) systems provide a useful framework for describing such open-system dynamics. A key feature of dissipation is asymmetric hopping, which leads to the non-Hermitian skin effect—an extreme sensitivity of eigenstates to boundary conditions. This mechanism can strongly modify many-body properties, as demonstrated in interacting systems and dissipation-induced phase transitions.

In non-Hermitian (NH) systems, exceptional points (EPs)—nonequilibrium singularities where eigenvalues and eigenstates coalesce—play a central role and lead to various anomalous phenomena, including enhanced responses and unconventional spectral structures. In many-body settings, EPs are also associated with nonequilibrium phase transitions in systems. However, realizing stable many-body phases hosting EPs remains challenging. In particular, NH fermionic superfluidity (NH-SF) exhibits EP-related reentrant phase transitions, but EPs appear only at phase boundaries where the superfluid becomes unstable [1, 2, 3]. This limitation makes it difficult to experimentally access EPs within the superfluid phase. Establishing mechanisms for stable NH-SF with accessible EPs is therefore crucial for understanding universal physical responses near EPs in NH many-body systems.

In this project, we study the NH attractive Hubbard model and show that spin depairing stabilizes a novel superfluid phase, termed exceptional fermionic superfluidity, characterized by both a finite order parameter and the presence of exceptional points (EPs). Using NH-BCS theory, we reveal that the interplay between EPs and an effective density of states governs its behavior [4, 5]. This phase exhibits distinct stability depending on the lattice geometry and provides a new route to realizing EPs in NH many-body systems.

## References

[1] K. Yamamoto, M. Nakagawa, K. Adachi, K. Takasan, M. Ueda, and N. Kawakami, Phys. Rev. Lett. 123, 123601 (2019).

[2] S. Takemori, K. Yamamoto, and A. Koga, Phys. Rev. B 109, L060501 (2024).

[3] S. Takemori, K. Yamamoto, and A. Koga, Phys. Rev. B 110, 184518 (2024).

[4] S. Takemori, K. Yamamoto, and A. Koga, Phys. Rev. Lett. 135, 266002 (2025).

[5] S. Takamori, K. Yamamoto, A. Koga, J. Low Temp. Phys. 222, 37 (2026).

# Theoretical study of magnetism in strongly-correlated electron systems: focus on $UTe_2$

Makoto SHIMIZU
*Department of Materials Engineering Science, The University of Osaka*
*Toyonaka 560-8531, Japan*

In strongly correlated systems, the ground state is sensitive to external parameters such as pressure and carrier doping, often leading to multiple competing orders that require a unified treatment of spin, orbital, and sublattice degrees of freedom. To address this problem, we investigate electronic and magnetic structures using density functional theory (DFT) and many-body methods.

*Magnetic fluctuations of $UTe_2$ at ambient and high pressure* [1].—$UTe_2$ is a heavy-fermion paramagnet and a strong candidate for spin-triplet superconductivity. While a close relationship between superconductivity and magnetic fluctuations has been implied, the microscopic mechanism of the magnetic fluctuations has not been clarified. In this study, we construct a 72-orbital model using DFT and investigate magnetic fluctuations at ambient and high pressure applying the random phase approximation (RPA). Large-scale parallel computations using more than one hundred nodes enabled calculations for the huge model. Our results for a 72-orbital effective model constructed from GGA+$U$ ($U$ = 1 eV) show good agreement with experimentally observed magnetic fluctuations and their pressure evolution.

*Magnetic fluctuations induced by quantum geometry* [2].—Magnetic fluctuations in multiband materials are often discussed in terms of Fermi-surface nesting and orbital (matrix-element) effects. However, their quantitative roles are not always clearly identified. In this study, based on a recently proposed formal decomposition of the static irreducible susceptibility into a dispersion (band) term and a wavefunction-geometry (quantum geometry) term, we implement this framework in first-principles-based tight-binding models. Applying this method to LaFeAsO and $Pb_9Cu(PO_4)_6O$, we analyze the contributions of these terms to magnetic fluctuations. The results indicate that the geometric term significantly affects the leading magnetic correlations: it enhances stripe-type antiferromagnetic correlations in LaFeAsO, while it suppresses antiferromagnetic fluctuations and stabilizes ferromagnetic tendencies in electron-doped $Pb_9Cu(PO_4)_6O$.

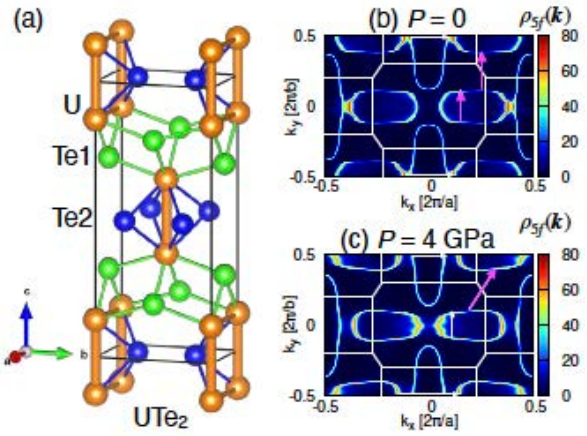


Figure 1: (a) Crystal structure of $UTe_2$. (b,c) Spectral weights of U-5$f$ states calculated within GGA+$U$ ($U$ = 1 eV). The magenta arrows show effective nestings corresponding to the antiferrmagnetic fluctuations with $\boldsymbol{Q} \parallel \boldsymbol{b}^*$.

*Pressure evolution of magnetic structure in nodal-line ferrimagnet $Mn_3Si_2Te_6$* [3].—

$Mn_3Si_2Te_6$ is a layered ferrimagnetic semiconductor with competing exchange interactions and strong magnetic anisotropy. Using DFT combined with Monte Carlo simulations, we investigate how external pressure modifies its electronic structure and magnetic couplings. The results reveal that pressure tunes the balance between ferromagnetic and antiferromagnetic interactions, leading to changes in magnetic order, anisotropy, and structural stability, thereby providing a microscopic understanding of pressure-induced phase transitions. Using ISSP supercomputing resources, we developed and employed Monte Carlo codes.

## References

[1] M. Shimizu and Y. Yanase, arXiv:2510.15322 [cond-mat.str-el].
[2] M. Shimizu, C.-g. Oh, and Y. Yanase, arXiv:2602.14511 [cond-mat.str-el].
[3] V. Venkatasubramanian, M. Shimizu, D. Guterding, and H. O. Jeschke, Commun. Mater. **7**, 94 (2026).

# Theoretical proposal of superconductivity in a hole-doped reduced bilayer nickelate $La_3Ni_2O_6$ : possibility of orbital space bilayer superconductivity

KAZUHIKO KUROKI
*Department of Physics, University of University*
*1-1 Machikaneyama, Toyonaka, Osaka, 560-0043, Japan*

The bilayer Hubbard model has been studied as a model where the superconducting $T_c$ can be higher than that of the $d$-wave superconducting state in the single-orbital Hubbard model [1, 2]. Hence, a realization of the bilayer Hubbard model in actual materials is a promissing path toward finding new high temperature superconductors. Along this path, we previously proposed that a double layer Ruddlesden-Popper compound $La_3Ni_2O_7$ can be a good candidate for realizing the bilayer Hubbard model that satisfies the above-mentioned conditions [3]. Recently, this material $La_3Ni_2O_7$ was found to exhibit high $T_c$ superconductivity with a highest $T_c$ of about 80 K under pressure [4].

On the other hand, our previous studies have shown that the multi-orbital Hubbard model is another example in which superconductivity is enhanced in the presence of an incipient band [5–7]. Although the bilayer Hubbard model involves only a single orbital with intraorbital interactions, the two-orbital Hubbard model comprises two orbitals per site and incorporates interorbital interactions. Despite these differences, in both models, superconductivity is optimized in the incipient-band regime [5]. The two models are mathematically equivalent when $U = U' = J = J'$ as shown in Ref. [8], where onsite interactions $U$, $U'$, $J$, and $J'$ are the intraorbital repulsion, interorbital repulsion, Hund's coupling, and pair hopping, respectively, with $2t_\perp$ in the bilayer model corresponding to the orbital level offset $\Delta E$ in the two-orbital model (see the middle of Fig. 1). In reality, $U > U' > J \sim J'$ and interorbital hybridization is present; nevertheless, our calculations in the two-orbital Hubbard model for a new type of cuprate $Ba_2CuO_{3+\delta}$ in Ref. [5] indicate that the correspondence between the bilayer and two-orbital models persists to some extent, and that superconductivity is enhanced with increasing $\Delta E$. Furthermore, we have found that the correspondence between the two models persists not only in the two-orbital model but also in the five-orbital model [6, 7]. Our calculations have shown that, even in the five-orbital system, superconductivity is enhanced by increasing the level offset $\Delta E$ between one orbital and the remaining four orbitals, and is optimized in the incipient-band regime.

Based on the correspondence between the bilayer and multi-orbital Hubbard models, we refer to the former as the real-space bilayer model (RSBM) and the latter as the orbital-space bilayer model (OSBM). $2t_\perp$ in the RSBM corresponds to $\Delta E$ in the OSBM.

Recently, in Ref.[9], we have investigated the possibility of superconductivity based on OSBM in a reduced bilayer nickelate $La_3Ni_2O_6$. We consider two types of structures, $T$ and $T'$, and performed band-structure calculations using three methods: GGA, GGA+$U$, and QSGW. We have shown that a large orbital level offset $\Delta E$ exists between the $d_{x^2-y^2}$ orbital and the other Ni-$d$ orbitals.

By analyzing superconductivity within FLEX calculations, we have found that $s\pm$-wave superconductivity can be enhanced by hole doping due to interorbital interactions in both the $T$ and $T'$ structures. This enhancement originates from the OSBM mechanism, where the Fermi level approaches the lower bands and the incipient-band situation is realized. Furthermore, we demonstrate that superconductivity is not significantly enhanced by the interorbital interaction between the $d_{x^2-y^2}$ and $d_{3z^2-r^2}$ orbitals alone; rather, it is enhanced by the interorbital interactions involving all four orbitals in the lower bands.

We have also shown that the energy difference between the $T$ and $T'$ structures varies under external hydrostatic pressure or internal pressure effects arising from differences in ionic radii, resulting in a shift of the stable structure. In addition, stable phonon dispersions are obtained under pressure in both the $T$ and $T'$ structures as shown in Fig.2. Considering that the insulating behavior at ambient pressure disappears under pressure, we consider the possibility of suppressing the insulating property and realizing OSBM-like superconductivity by applying pressure and hole doping.

[1] K. Kuroki, T. Kimura, and R. Arita, Phys. Rev. B **66**, 184508 (2002).
[2] T. A. Maier and D. J. Scalapino, Phys. Rev. B **84**, 180513(R) (2011).
[3] M. Nakata, D. Ogura, H. Usui, and K. Kuroki, Phys. Rev. B **95**, 214509 (2017).
[4] H. Sun, M. Huo, X. Hu, J. Li, Z. Liu, Y. Han, L. Tang, Z. Mao, P. Yang, B. Wang, J. Cheng, D.-

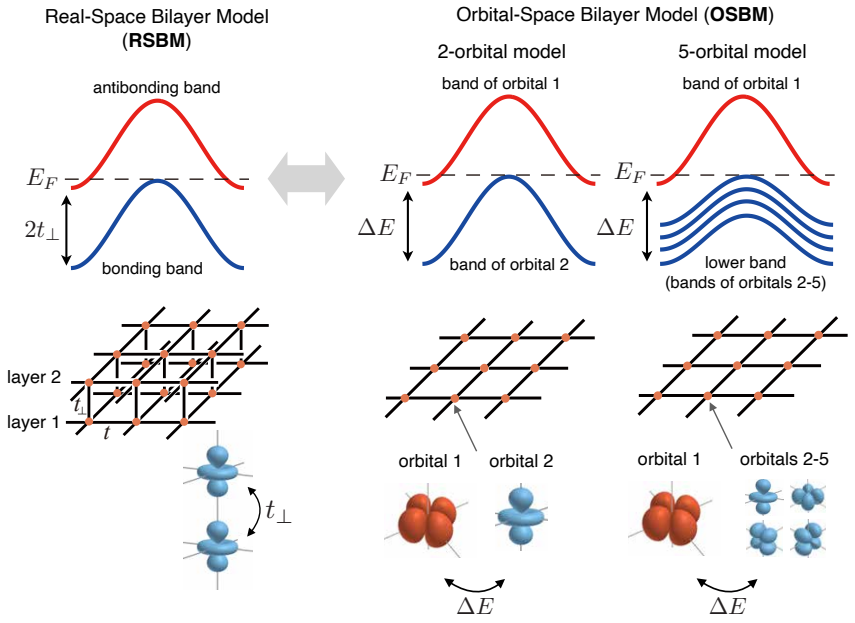


FIG. 1. Schematics of the Real-Space Bilayer Model (RSBM) and the Orbital-Space Bilayer Model (OSBM). The interlayer hopping $t_\perp$ in the RSBM gives rise to bonding and antibonding bands with an energy separation of $2t_\perp$. In the OSBM, orbital-level offsets $\Delta E$ between multiple orbitals play an analogous role. In both models, superconductivity is optimized in the incipient-band regime, where one band intersects the Fermi level while the other touches or lies slightly away from it. The correspondence between RSBM and OSBM has been examined also in multi-orbital systems, such as the five-orbital model.

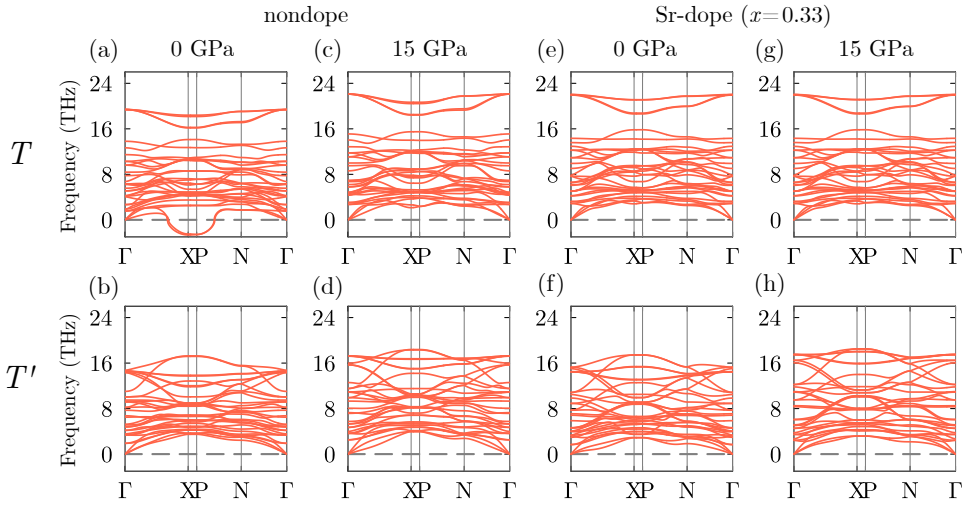


FIG. 2. The phonon dispersions of (a)–(d) non-doped $La_3Ni_2O_6$ and (e)–(h) Sr-doped $(La_{1-x}Sr_x)_3Ni_2O_6$ ($x = 0.33$) for both the $T$ and $T'$ structures under pressures of $P = 0$ and 15 GPa.

X. Yao, G.-M. Zhang, and M. Wang, Nature **621**, 493 (2023).
[5] K. Yamazaki, M. Ochi, D. Ogura, K. Kuroki, H. Eisaki, S. Uchida, and H. Aoki, Phys. Rev. Res. **2**, 033356 (2020).
[6] N. Kitamine, M. Ochi, and K. Kuroki, Phys. Rev. Res. **2**, 042032(R) (2020).
[7] H. Sakakibara, R. Mizuno, M. Ochi, H. Usui, and K. Kuroki, Phys. Rev. B **111**, 224511 (2025).
[8] H. Shinaoka, Y. Nomura, S. Biermann, M. Troyer, and P. Werner, Phys. Rev. B **92**, 195126 (2015).
[9] S. Kamiyama, R. Kohno, Y. Hoshi, K. Ushio, D. Nakaoka, H. Sakakibara, and K. Kuroki, (2026), arXiv:2603.11771.

# Control of transverse and longitudinal spin fluctuations in intermediately correlated systems

Hidemaro SUWA
*Department of Physics, University of Tokyo, Tokyo 113-0033*

Spin fluctuations underpin emergent quantum phenomena from unconventional superconductivity to quantum spin liquids. Their transverse (TSF, orientational) and longitudinal (LSF, amplitude) components are conventionally treated as independent, but whether they are correlated in real materials—particularly in the intermediately correlated regime bridging Slater and Mott limits—had remained an open question. We addressed this both experimentally and theoretically, using bilayer iridate superlattices $[(SrIrO_3)_2/(Sr_{1-x}Ca_xTiO_3)_1]_{20}$ as a tunable $J_{\mathrm{eff}} = 1/2$ platform [1].

The theoretical core is a magnetic phase diagram computed as a function of in-plane and out-of-plane octahedral rotations. Contrary to the long-held view that bilayer iridates host a robust $c$-axis Ising anisotropy, the calculation shows that a sufficiently strong out-of-plane rotation drives a $c$- to $a$-axis antiferromagnetic transition. A symmetry analysis identifies the emergent in-phase rotation about the $a$-axis as the responsible order parameter: the rotated mirror plane (normal to $a$) pins the easy axis along $a$, in close analogy to—yet rotated 45° from—the single-layer iridate case. This furnishes a microscopic, symmetry-based link between octahedral distortion and Néel-vector reorientation. Experimentally, Ca substitution in the spacer continuously tunes the in-phase rotation, realizing the predicted anisotropy competition; TSF is consequently maximized near $x \approx 0.5$.

A second theoretical thread interprets magnetotransport at $T_{\mathrm{N}}$ within the intermediately correlated framework, where local moments arise from particle–hole pair formation. LSF then corresponds to thermally excited particle–hole pairs, suppressed by an external field and producing the linear, positive in-plane magnetoresistance (MR) observed in all samples. The strength of this signal tracks the effective correlation, which varies non-monotonically with $x$ and is minimized at $x \approx 0.25$—precisely opposite to TSF. TSF instead drives field-suppressed carrier scattering with a negative, parabolic MR; this hallmark emerges only out-of-plane near $x = 0.25$.

To analyze this material theoretically, we performed large-scale semiclassical calculations of the bilayer iridate system for various octahedral rotation parameters on ISSP System B in the class C project (2025-Ca-0113) using MPI parallelization on up to 10 nodes simultaneously. Our work establishes that TSF and LSF are tied through the effective electronic correlation and modulate in approximately opposite ways across the phase diagram. More broadly, it shows that artificial crystalline engineering can independently target distinct components of the spin-fluctuation spectrum, opening a controllable route to designing complex magnetic states and probing the spin dynamics relevant to unconventional superconductivity.

## References

[1] E. Men et al., *Newton* **2**, 100483 (2026).

# Photoinduced Nonequilibrium Dynamics in the Charge-Ordered Phase of Doped Mott Insulators

Takami TOHYAMA
*Department of Applied Physics, Tokyo University of Science, Katsushika, Tokyo 125-8585*

The dynamics of holes doped into a Mott insulator induce both Drude and finite-frequency absorptions within the Mott gap in the optical conductivity. In cuprate superconductors, a broad mid-infrared (mid-IR) absorption around 0.5 eV has been observed. The origin of this mid-IR absorption is generally attributed to a mixture of charge, lattice, and magnetic excitations. Similar broad mid-IR features also appear in two-leg ladder cuprates.

Recent advances in laser technology have enabled ultrashort pump pulses to be tuned to the Drude and mid-IR absorption regions. Indeed, mid-IR pulses have already been applied to cuprate superconductors. In the doped two-leg ladder Mott insulator $Sr_{14-x}Ca_xCu_{24}O_{41}$, which exhibits a tendency toward charge ordering, photo-pumping and pump–probe spectroscopy have been investigated. However, the pump energies used so far lie near the edge of the Mott gap. Thus, it remains an open question how pump pulses tuned directly to the Drude and mid-IR absorptions influence the low-energy charge dynamics in strongly correlated metals with charge order. In particular, theoretical predictions regarding the differences between Drude pumping and mid-IR pumping will be valuable for guiding future experimental studies in these systems.

To address this issue, we investigate the effects of photo-pumping on doped Mott insulators using few-cycle laser pulses with energies corresponding to the Drude and mid-IR absorption regions, and predict how the optical conductivity is modified by the pump [2]. As representative models of strongly correlated metals with a tendency toward charge order (such as charge stripes), we employ a two-leg Hubbard ladder and a four-leg $t$-$J$ ladder. The optical conductivity after pumping is computed using the time-dependent density matrix renormalization group (tDMRG) implemented with Legendre polynomials [1]. We use two target states at times $t$ and $t+\delta t$ to construct a basis capable of representing wavefunctions in the time-dependent Hilbert space. This two-target tDMRG procedure enables accurate evaluation of time-dependent observables even when the Hamiltonian varies rapidly in time.

We find that a monocycle electric-field pulse tuned to the Drude absorption reduces the Drude weight and slightly enhances the mid-IR spectral weight, although this enhancement diminishes as the pulse intensity increases. In contrast, pumping at the mid-IR absorption leaves the mid-IR weight unchanged and only reduces the Drude weight. This behavior arises because the mid-IR absorption originates from magnetic excitations rather than charge order. These predictions can be tested experimentally by applying ultrashort low-energy pump pulses to cuprate materials.

## References

[1] K. Shinjo, S. Sota, and T. Tohyama: Phys. Rev. Res. **4**, L032019 (2022).

[2] S. Chandra, K. Shinjo, S. Sota, S. Yunoki, and T. Tohyama: Phys. Rev. B **113**, 045127 (2026).

# First-principles and machine-learning study of pressure-dependent structures and electronic states in organic molecular conductors

Kazuyoshi YOSHIMI
*Institute for Solid State Physics, The University of Tokyo*
*Kashiwa-no-ha, Kashiwa, Chiba 277-8581*

Organic molecular conductors are a useful platform for studying pressure-tuned strongly correlated electron systems: charge order, Mott insulating states, Dirac electronic states, and unconventional superconductivity can be controlled by modest changes in lattice geometry. At the same time, their soft van der Waals packing makes first-principles structure prediction demanding, since small errors in the relaxed structure propagate into the bandwidth, Fermi surface, and effective Coulomb interactions. In project 2025-Ca-0011 we used the ISSP supercomputer to address three related topics: (i) the pressure-induced Mott-insulator-to-superconductor crossover in $\beta'$-(BEDT-TTF)$_2$ICl$_2$, (ii) the identification of an ambient-pressure organic Dirac electron system, and (iii) a systematic benchmark of dispersion corrections and machine-learning potentials (MLPs) for pressure-dependent molecular crystal structures.

**Pressure-induced Fermi-surface change in $\beta'$-(BEDT-TTF)$_2$ICl$_2$.** $\beta'$-(BEDT-TTF)$_2$ICl$_2$ shows the highest reported superconducting transition temperature among molecular organic superconductors, $T_c$ = 14.2 K at 8.2 GPa. To clarify its pressure-induced electronic evolution, we combined synchrotron X-ray crystallography with plane-wave DFT structure relaxation in Quantum ESPRESSO[6] up to 11 GPa, with the systematic parameter sweeps managed by the bulk-job utility Moller[7], as reported in Ref. [1]. Low-energy effective models were then derived by cRPA using RESPACK[3], and their electronic instabilities analysed with the mean-field/RPA solver H-wave[4]. The pressure-induced structural deformation reorganises the Fermi surface in a Lifshitz-type manner, accompanying the crossover from a Mott insulating state to the metallic and superconducting regime[1]. A comparison between dispersion-uncorrected DFT and the experimental structures also revealed a small but systematic change in the BEDT-TTF dimer geometry, which motivated the broader benchmark of dispersion treatments below.

**Ambient-pressure Dirac electrons in $\alpha$-(BETS)$_2$AuCl$_2$.** As a chemical-pressure analogue of high-pressure $\alpha$-(ET)$_2$I$_3$, we identified $\alpha$-(BETS)$_2$AuCl$_2$ as a quasi-three-dimensional massive Dirac semimetal at ambient pressure[2]. Transport measurements show a large positive in-plane magnetoresistance and an anomalous negative interlayer magnetoresistance. First-principles calculations including spin–orbit coupling, performed on the ISSP system, reproduce the band crossing and residual Fermi pocket and clarify that the Au–Cl anion layer plays an essential role in stabilising the quasi-3D Dirac dispersion. This establishes $\alpha$-(BETS)$_2$AuCl$_2$ as a clean ambient-pressure platform for spectroscopic and transport studies of organic Dirac fermions.

**Benchmarking dispersion corrections and MLPs for pressure-dependent structures.** The structural sensitivity found in $\beta'$-(BEDT-TTF)$_2$ICl$_2$ prompted a systematic benchmark of structure-relaxation protocols for soft molecular crystals. We compared foundation-model MLPs (ORB, MACE, CHGNet, MatterSim, SevenNet) combined with several dispersion treatments (DFT-D3(BJ) with different damping functions and DFT-D4), against the experimental pressure-dependent crystal structures of three charge-transfer salts: $\beta'$-(BEDT-TTF)$_2$ICl$_2$, (TMTTF)$_2$PF$_6$, and (TMTTF)$_2$SbF$_6$, with more than ten pressure points each up to $\sim$ 10 GPa. The equation of state was obtained by fitting the relaxed volumes to a third-order Birch–Murnaghan form. The trends so far indicate that the dispersion-correction protocol, in particular the damping function, affects the predicted equation of state as strongly as, or more strongly than, the MLP architecture, and that the 2D-dimer compound $\beta'$-(BEDT-TTF)$_2$ICl$_2$ is systematically softer than experiment for every protocol tested, in contrast to the 1D-stack TMTTF salts. To disentangle MLP-intrinsic errors from those inherited from the underlying DFT functional, reference plane-wave DFT calculations (PBEsol+D3 and PBE without dispersion correction) are now in progress on the ISSP system.

**Outlook.** Building on our recent ab initio survey of the quasi-one-dimensional (TMTTF)$_2$X family[5], we will convert the relaxed structures into Wannier-based tight-binding models and cRPA effective interactions, and quantify how structural uncertainty from the dispersion treatment propagates into transfer integrals, the Mott $U/W$ ratio, and the resulting phase diagrams of $\beta'$-(BEDT-TTF)$_2$ICl$_2$, (TMTTF)$_2$X, and $\alpha$-(BETS)$_2$AuCl$_2$. The resulting dataset will also serve as a reference for evaluating the next generation of pressure-aware MLPs for soft molecular crystals.

## References

[1] T. Kobayashi, K. Yoshimi, H. Ma, S. Sekine, H. Taniguchi, N. Matsunaga, A. Kawamoto, and Y. Uwatoko, Phys. Rev. Materials **9**, L021801 (2025).

[2] T. Kobayashi, K. Yoshimi, A. Nishimoto, S. Michimura, and H. Taniguchi, J. Phys. Soc. Jpn. **95**, 043701 (2026).

[3] K. Nakamura, Y. Yoshimoto, Y. Nomura, T. Tadano, M. Kawamura, T. Kosugi, K. Yoshimi, T. Misawa, and Y. Motoyama, Comput. Phys. Commun. **261**, 107781 (2021).

[4] T. Aoyama, K. Yoshimi, K. Ido, Y. Motoyama, T. Kawamura, T. Misawa, T. Kato, and A. Kobayashi, Comput. Phys. Commun. **298**, 109087 (2024).

[5] K. Yoshimi, T. Misawa, T. Tsumuraya, and H. Seo, Phys. Rev. Lett. **131**, 036401 (2023).

[6] P. Giannozzi, O. Andreussi, T. Brumme *et al.*, J. Phys. Condens. Matter **29**, 465901 (2017).

[7] https://github.com/issp-center-dev/Moller.

# Nonequilibrium phenomena in strongly correlated systems

Robert Peters and Tsuneya Yoshida

*Kyoto University, Kyoto 606-8501*

We have studied nonequilibrium and nonlinear response phenomena in strongly correlated systems using large-scale numerical simulations on the ISSP supercomputer system. In particular, we focused on correlation effects in altermagnetic systems and on the stability of topological phases under generic perturbations.

First, we investigated the nonlinear magnetoelectric effect (NMEE) in a correlated altermagnetic system within a self-consistent dynamical mean-field theory (DMFT) framework. The lattice model was mapped onto an effective quantum impurity problem, which was solved using the numerical renormalization group, allowing us to access real-frequency spectral functions and response functions with high resolution. Based on the interacting Green's functions, we computed the optical conductivity and the frequency-dependent nonlinear magnetoelectric response over a wide range of interaction strengths and temperatures. The calculations reveal that the NMEE is directly controlled by the spin-resolved spectral structure of the correlated system. In particular, the low-frequency response is dominated by electronic states near the Fermi energy, indicating a Fermi-surface origin of the nonlinear response. Furthermore, we find a strong enhancement of the response in the vicinity of an interaction-driven phase transition [see Fig. 1], where coherent quasiparticles and enhanced spin contrast lead to a large nonlinear signal, while thermal fluctuations suppress the response due to increased scattering and reduced spin polarization. These results were obtained through self-consistent DMFT calculations and systematic parameter scans in interaction strength, temperature, and frequency, which required substantial computational resources on the ISSP system. The results are currently under preparation for publication.

In parallel, we performed variational simulations of a quantum spin model using neural-network quantum states (NQS). Specifically, we studied the toric code subject to an isotropic antiferromagnetic Heisenberg perturbation and analyzed the resulting breakdown of topological order. The ground state was obtained using variational Monte Carlo with a symmetry-adapted neural-network ansatz, allowing us to access system sizes beyond exact diagonalization. We identified the quantum phase transition by analyzing the fidelity susceptibility, non-contractible Wilson loop operators, and topological entanglement entropy. In the weak-coupling regime, the numerical results are in excellent agreement with an effective low-energy description derived from a

Schrieffer–Wolff transformation, while at intermediate coupling the topological phase is destroyed and replaced by a magnetically ordered state. These simulations were partially carried out on GPU resources of the ISSP system, enabling efficient optimization of the neural-network wave function.

Overall, the combination of DMFT and neural-network-based approaches provides a complementary framework to investigate correlation-driven phenomena in quantum many-body systems, ranging from nonlinear response in itinerant systems to the stability of topological phases in spin models.

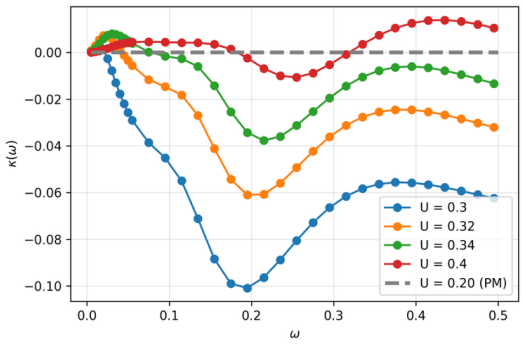


*Figure 1: Frequency dependence of the nonlinear magnetoelectric response κ(ω) for different interaction strengths*

## References

[1] W. Jang, R. Peters, and T. Posske, "*The toric code under antiferromagnetic isotropic Heisenberg interactions*," arXiv:2603.05707.

# Numerical calculations of gapped spin orders in low dimensional systems

Yasuhiro Tada

*Quantum Matter Program, Graduate School of Advanced Science and Engineering, Hiroshima University, Higashihiroshima, Hiroshima 739-8530*

We have studied gapped spin orders in low dimensional quantum systems. The first system is a quantum spin system on a square lattice [1]. In this system, there are two kinds of interactions, the conventional XY interaction and the chirality interaction. We use infinite density matrix renormalization group and consider infinite cylinder geometry. In this setup, the ground state is a gapless Tomonaga-Luttinger liquid for a range of the chiral interaction, while it is a gapped chiral spin liquid when the chiral interaction is large. We demonstrate that both of the gaplessness and the gappedness can be well detected by the polarization amplitude $|z^2|$. Indeed, we find that $|z^2| \sim L^{-\alpha} \to 0$ in the gapless phase in the thermodynamic limit, where $\alpha$ is an exponent which depends on the model parameter. On the other hand, $|z^2| \sim e^{-c/L}$ in the gapped state, where $c$ is a positive constant. This is the first numerical demonstration that the polarization amplitude works for the two dimensional gapped order realized in quasi-one dimensional geometry.

The second system is the S=3/2 Kondo-Heisenberg chain [2]. At half-filling, the system is a Kondo insulator where there exist unscreened spins realizing the topological Haldane state. It was previously argued that, away from half-filling, there is a spin gapped system where the pair-density-wave correlation is enhanced. We show that the pair-density-wave order is indeed the dominant order among several candidate orders. Interestingly, the pair-density-wave correlation shows anomalous behaviors around the edges of the system in sharp contrast to the standard S=1/2 system. Therefore, the charge sector may be regarded as a topological state in this specific sense. On the other hand, the spin correlation exhibits no signature of an edge mode, which implies that the spin sector is not a topological state.

## References

[1] T. Yokoyama and Y. Tada, arXiv: 2602.12990.

[2] H. Hirose, S. C. Furuya, and Y. Tada, in preparation.

# Microscopic Simulations of Electron-Phonon Dynamics in Mott Insulators

Rico Pohle

*Faculty of Science, Shizuoka University, Shizuoka 422-8529*

We have developed a computational framework for simulating the nonequilibrium dynamics of strongly correlated Mott insulators, overcoming key limitations of conventional approaches in treating many-body interactions and energy dissipation on equal footing [1].

The method combines concepts from quantum field theory with condensed matter to provide a microscopic description of local electronic degrees of freedom and their coupling to lattice vibrations (phonons) and an external thermal bath.

It enables simulations of energy flow from correlated electrons to phonons and ultimately to the environment, thereby capturing dissipation and relaxation processes within a microscopic framework, in contrast to approaches such as Landau–Lifshitz–Gilbert (LLG) dynamics, where dissipation is introduced phenomenologically.

Numerically, the approach requires solving large sets of coupled stochastic differential equations for electronic and phononic degrees of freedom across extended lattices and long time scales. These simulations are computationally demanding and were carried out using high-performance computing resources.

As a proof of concept, we performed large-scale simulations of a two-orbital spin chain, demonstrating nontrivial hybridization between spin and phonon excitations in the dynamical spectra. The results highlight how electron–phonon coupling qualitatively modifies collective modes and energy transport in strongly correlated systems.

## References

[1] R. Pohle, Y. Motome, T. Tadano, and S. Hoshino, preprint (arXiv:2507.19764).

# Vison control driven by lattice deformation in Kitaev quantum spin liquids

Joji NASU
*Department of Physics, Tohoku University*
*Sendai 980-8578*

Quantum spin liquids (QSLs) host emergent fractionalized excitations and gauge degrees of freedom, providing a unique platform for studying nontrivial quantum phenomena. The Kitaev model is a paradigmatic example of such a system, in which spins are fractionalized into itinerant Majorana fermions and localized $Z_2$ gauge fluxes (visons) [1]. Although the model is exactly solvable and exhibits rich physics, its highly symmetric structure imposes a fundamental limitation: in the isotropic Kitaev limit, the system lacks an intrinsic directional bias and therefore does not allow controlled manipulation of vison positions along a specific spatial direction.

To establish a mechanism for directional control of visons within the framework of the Kitaev model, we investigate the effects of interaction anisotropy and triaxial lattice strain. In the present study, we calculate the time evolution of the Kitaev QSL in the presence of an excited vison using time-dependent mean-field theory [2, 3]. In the calculations, we use a parallel computing via the intel Math Kernel Library to handle the large system sizes required for accurate simulations of vison dynamics.

To elucidate the role of interaction anisotropy, we first perform a quantitative analysis of vison dynamics under a locally applied magnetic field. Our results demonstrate that increasing the interaction strength along the bond direction corresponding to the desired control direction significantly enhances vison mobility. In particular, a relatively weak magnetic field becomes sufficient to induce the motion of an excited vison when the interaction anisotropy is sufficiently strong. This clearly indicates that vison displacement is strongly governed by the magnitude of the bond-dependent interaction along the direction of motion.

Next, we investigate whether directional control can be achieved solely through lattice deformation, without relying on spatially inhomogeneous magnetic fields. Using triaxial strain introduced in the theoretical model, we perform numerical simulations in which the strain magnitude and orientation are systematically varied. We find that when strain is applied in a direction that breaks translational symmetry along the intended propagation direction, the vison exhibits finite displacement even under a spatially uniform magnetic field. This demonstrates that symmetry breaking induced by strain plays a crucial role in enabling controlled vison dynamics.

## References

[1] A. Kitaev, , Ann. Phys. (NY) **303**, 2 (2003).

[2] C. Harada, A. Ono, and J. Nasu, Phys. Rev. B **108**, L241118 (2023).

[3] C. Harada, A. Ono, and J. Nasu, Phys. Rev. B **110**, 214426 (2024).

# Computational study on two-particle responses in correlated altermagnets using DFT+DMFT method

Atsushi Hariki

*Department of Physics and Electronics,*

*Osaka Metropolitan University, 1-1 Gakuen-cho, Naka-ku, Sakai, Osaka 599-8531, Japan*

We carried out a computational study of resonant inelastic x-ray scattering (RIXS) in candidate altermagnetic materials using DFT+DMFT (density functional theory plus dynamical mean-field theory). Altermagnets have recently revitalized interest in collinear antiferromagnets owing to their unique electronic structure, which breaks time-reversal symmetry despite exhibiting compensated magnetic moments. However, experimentally established altermagnetic materials remain limited, and new experimental techniques capable of detecting the associated symmetry breaking are desirable.

In this project, we explore RIXS as a probe to characterize altermagnetism and to gain insight into two-particle excitations as well as domain structures. At the transition-metal *L*-edge, RIXS involves the resonant excitation of a 2*p* core electron into 3*d* valence states, followed by de-excitation, and is described as a coherent second-order process within the Kramers–Heisenberg formalism. We simulated candidate materials (MnTe and $Fe_2Mo_3O_8$) using our in-house DFT+DMFT and atomic multiplet codes [1]. This is supported by large-scale parallel computations at ISSP, enabling a systematic scan of the incident x-ray energy, which serves as a tuning parameter in the RIXS experiments.

For MnTe, we have shown that altermagnetic domains can be probed by analyzing circular dichroism (CD) in RIXS [2], as demonstrated by direct comparison between recent experimental data and our DFT+DMFT calculations. $Fe_2Mo_3O_8$ is unique among candidate materials in that it hosts two fundamental altermagnetic units, namely octahedral and tetrahedral Fe sites, within its crystal structure. To resolve the altermagnetic symmetry breaking on each unit, our numerical calculations predict distinct CD features at specific energy ranges in the RIXS spectra that can be uniquely attributed to each site. The simulated results are consistent with recent experimental observations for this compound [3].

## References

[1] A. Hariki *et al*., Phys. Rev. B **101**, 115130 (2020).

[2] D. Takegami *et al*., Phys. Rev. Lett. **135**, 196502 (2025).

[3] G. Channagowdra *et al*., arXiv: 2512.00737

# Computational Study of Magnetic Circular Dichroism in Resonant Inelastic X-ray Scattering Spectra of Strongly Correlated Materials

Atsushi Hariki

*Department of Physics and Electronics,*

*Osaka Metropolitan University, 1-1 Gakuen-cho, Naka-ku, Sakai, Osaka 599-8531, Japan*

Altermagnets have recently emerged as a new class of collinear magnets that host time-reversal-symmetry–broken electronic structures while retaining compensated magnetic moments, similar to conventional antiferromagnets in the non-relativistic limit. However, experimentally well-established altermagnetic materials remain limited, mainly because the available probes to identify the symmetry breaking associated with altermagnetism are still scarce.

We conducted computational simulations of circular dichroism (CD) in resonant inelastic X-ray scattering (RIXS) for several candidate altermagnets (MnTe, CrSb, and $NiF_2$) using our in-house DFT+DMFT (density functional theory plus dynamical mean-field theory) and atomic multiplet codes, together with large-scale parallel computing resources provided by ISSP. RIXS is a complex, coherent second-order optical process, involving core-electron excitation into the valence *d* shell followed by de-excitation, and is described by the Kramers–Heisenberg formalism. We utilized the ISSP facility to efficiently map out the incoming X-ray energies, which serve as a tunable parameter and can be naturally parallelized [1].

We have confirmed strong CD signals in several candidate altermagnets. Notably, these signals appear even in cases where X-ray magnetic circular dichroism (XMCD) is forbidden by symmetry, indicating that RIXS-CD can be used more broadly to probe altermagnetism. Furthermore, we have established selection rules for RIXS-CD, supported by these numerical calculations [2].

In addition, we investigated the electronic structures of $UTe_2$ [3] using the DFT+DMFT method.

## References

[1] A. Hariki *et al*., Phys. Rev. B **101**, 115130 (2020).

[2] M. Furo *et al*., Phys. Rev. B **112**, 214429 (2025).

[3] M. Sundermann *et al*., Phys. Rev. Research **7**, 043195 (2025).

# Quantum many-body wave function in strongly correlated electrons

Takashi YANAGISAWA
*National Institute of Advanced Industrial Science and Technology (AIST)*
*1-1-1 Umezono, Tsukuba, Ibaraki 305-8568, Japan*

## 1 On numerical calcualtions

The formulation of many-body wave functions is significantly important in the study of strongly correlated electron systems. In our numerical approach, we proposed an optimized many-body wave function to take account of strong correlation between electrons. The expectation values are evaluated by using the Metropolis Monte Carlo procedure. We carried out parallel computations in Monte Carlo calculations. In order to reduce statistical errors, we performed $\sim 500$ parallel calculations since parallel computing is very essential to reduce Monte Carlo statistical errors. The parallelization rate of our programs is over 99%.

## 2 Introduction

The many-body wave function can be written as

$$\psi = e^{-\Delta\tau K} e^{-\Delta\tau V} \cdots e^{-\Delta\tau K} e^{-\Delta\tau V} \psi_0, \quad (1)$$

where $K$ and $V$ are kinetic and interaction part of the Hamiltonian, respectively, and $\psi_0$ is an initial one-body wave function. We generalize this wave function in the form

$$\psi_M = e^{-\lambda_M K} e^{-\alpha_M V} \cdots e^{-\lambda_1 K} e^{-\alpha_1 V} \psi_0, \quad (2)$$

where $\lambda_j$ and $\alpha_j$ $(j = 1, \cdots, M)$ are parameters. $\psi_M$ will approach the ground state when $M$ is large enough.

We consider the two-dimensional Hubbard model with the on-site repulsive interaction $V = U \sum_i n_{i\uparrow} n_{i\downarrow}$. $P_G(\alpha) \equiv e^{-\alpha V}$ is identified as the Gutzwiller operator that controls the double occupancy with the variational parameter $g = e^{-\alpha U}$[1]. Let us examine the following wave functions. $\psi^{(1)} \equiv \psi_G = P_G \psi_0$ is the well known Gutzwiller wave function. $\psi^{(2)} \equiv \exp(-\lambda_1 K) P_G \psi_0$ is for $M = 1$, where $\psi_0$ indicates an initial wave function which is usually taken as the Fermi sea, the BCS wave function or the state with some magnetic (or charge) orders.

We can also consider $\psi^{(3)} \equiv P_G(g_2)\psi^{(2)}$ and $\psi^{(4)} \equiv \exp(-\lambda_2 K) P_G(g_2) \psi^{(2)}$ for different variational parameters $\lambda_2$ and $g_2$. The wave function $\psi^{(4)}$ is a very good many-body wave function because the ground-state energy is lowered greatly and the ground-state energy is lower than those that are evaluated by using any other wave functions. We can further proceed to employ $\psi^{(\ell)}$ with larger $\ell$.

## 3 Pair correlation function and the Gutzwiller effect

We have carried out variational Monte Carlo simulations to examine the ground state of the two-dimensional Hubbard model on a square lattice. We here examine the effect of strong correlation on superconductivity. The BCS wave function $\psi_{BCS}(\Delta_s)$ with the gap function $\Delta_s$ clearly shows the long-range correlation. In Fig. 1, we show the $d$-wave superconducting (SC) correlation function $D_{sc}(\ell) = \langle \Delta^\dagger(i) \Delta(i+\ell) \rangle$ as a function of lattice sites for $N_e = 128$, $U = 18t$ and $t' = 0$ on a $12 \times 12$ lattice[6]. Here the pair annihilation operator $\Delta(i)$ at the site $i$ is given by

$$\Delta(i) = \Delta_x(i) + \Delta_{-x}(i) - (\Delta_y(i) + \Delta_{-y}(i)), \quad (3)$$

where $\Delta_{\hat{\alpha}} = c_{i\downarrow} c_{i+\hat{\alpha}\uparrow} - c_{i\uparrow} c_{i+\hat{\alpha}\downarrow}$ for $\alpha = x$ and $y$. $\hat{\alpha}$ indicates the unit vector in the $\alpha$-th direction. The pair correlation function $D_{sc}(\ell)$

shows that the long-range order of superconductivity indeed exists in the ground state.

The correlation function $D_{sc}(\ell)$ is, however, reduced by the Gutzwiller operator as shown in Fig. 1 where the Gutzwiller projection operator suppresses the pair correlation considerably. In Fig. 2 we show the expectation value of the superconducting order parameter as a function of the Gutzwiller parameter $1-g$. The strong electron correlation induces the anisotropic pairing and at the same time the pair correlation function is suppressed by the *Gutzwiller effect* caused by $P_G$. In particular, when $g$ is small, the *Gutzwiller effect* makes the pair correlation function very small. Thus the effect of the Gutzwiller operator might be described as a double-edged sword for superconductivity.

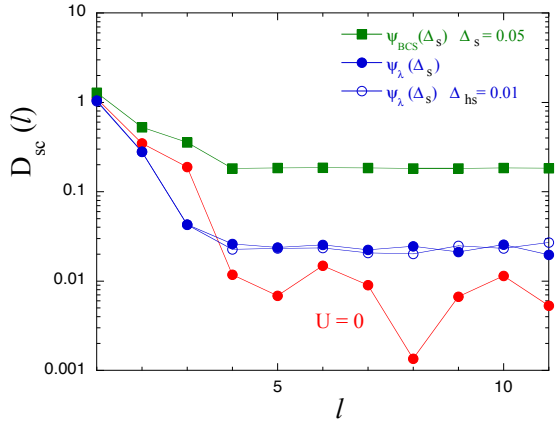


Figure 1: The pair correlation function $D_{sc}(\ell)$ as a function of the lattice site $\ell$ on a $12 \times 12$ lattice with $U = 18t$, $t' = 0$ and $N_e = 128$ for $\psi_\lambda = \psi^{(2)}$. The lattice sites $\ell$ are $\ell$=(1,1), (1,2), (1,3), (1,4), (1,5), (1,6), (2,6), (3,6), (4,6), (5,6) and (6,6) and the site $i$ is chosen as $i = (1,1)$. We show $D_{sc}(\ell)$ for $\psi_\lambda$ with the SC order parameter $\Delta_s = 0.05$. The figure also includes $D_{sc}(\ell)$ for $U = 0$ (red circles) and that for the non-interacting BCS wave function with $\Delta_s = 0.05$. We also show the result for $\psi_\lambda$ with an additional variational parameters $\Delta_{hs}$ which is the gap parameter introduced in the kinetic term $K$.

As a summary, we examined the ground state of the two-dimensional Hubbard model by using the optimized many-body wave function $\psi_M$. We will proceed further for larger $M$ values.

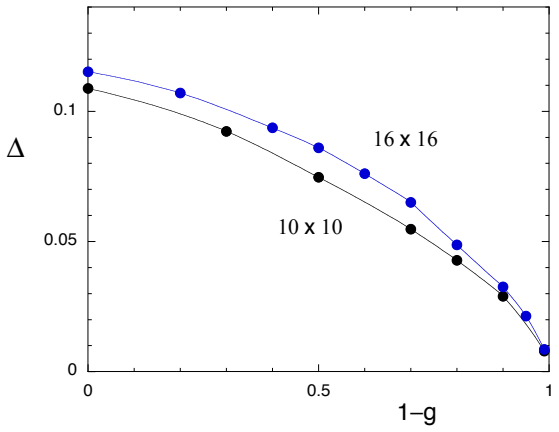


Figure 2: The expectation value of SC order parameter $\Delta \equiv \Delta_s$ as a function of the Gutzwiller parameter $1-g$ for the BCS-Gutzwiller wave function $P_G\psi_{BCS}$ on $10 \times 10$ and $16 \times 16$ lattices, with $U = 18t$, $t' = 0$ and $N_e = 128$. We set $N_e = 88$ on $10 \times 10$ and $N_e = 128$ on $16 \times 16$ lattice.

## References

[1] T. Yanagisawa et al., J. Phys. Soc. Jpn. 67, 3867 (1998).
T. Yanagisawa, Phys. Rev. B75, 224503 (2007) (arXiv: 0707.1929).

[2] T. Yanagisawa, J. Phys. Soc. Jpn. 85, 114707 (2016).
T. Yanagisawa, J. Phys. Soc. Jpn. 88, 054702 (2019).
T. Yanagisawa, Condensed Matter 4, 57 (2019).

[3] T. Yanagisawa, Phys. Lett. A403, 127382 (2021).
T. Yanagisawa et al., EPL 134, 27004 (2021).

[4] M. Miyazaki, T. Yanagisawa, Phys. Lett. A448, 128276 (2022).

[5] T. Yanagisawa, High Temperature Materials 1, 10004 (2024).

[6] T. Yanagisawa, J. Phys. Soc. Jpn. 94, 074708 (2025).

# Computing nonlinear response functions via time evolution

Atsushi Ono
*Department of Physics, Graduate School of Science, Tohoku University*
*Sendai 980-8578*

In recent years, there has been growing interest in nonlinear responses in condensed matter systems, and calculating nonlinear response functions is essential for understanding them. Although real-time evolution calculations incorporate response contributions of all orders, a general theory for reconstructing response functions of a specific order from such calculations had not been established.

In Ref. [1], we proposed a general framework for computing nonlinear response functions through real-time simulations. In general, the $n$th-order frequency response function of a physical quantity $Q$ to an external field $f$ is defined by the functional derivative

$$\bar{\chi}^{(n)}(\omega_1,\ldots,\omega_n) = \frac{(2\pi)^{n-1}}{f(\omega_n)} \frac{\delta^{n-1}\langle Q\rangle^{(n)}(\omega)}{\delta f(\omega_{n-1})\cdots\delta f(\omega_1)}, \quad (1)$$

where $\omega_n = \omega - \sum_{i=1}^{n-1}\omega_i$. In this theory, this functional derivative is numerically evaluated from time-evolution calculations performed under multiple external fields whose phases and amplitudes are appropriately controlled. This framework is, in principle, applicable to a wide variety of methods capable of simulating the real-time dynamics of quantum or classical systems.

As a proof of concept, we calculated the second- and third-order optical response functions in the Rice–Mele model (Fig. 1). The results obtained using this theory, shown by the red solid lines, were confirmed to accurately reproduce those obtained by conventional perturbation theory. We also analyzed a strongly correlated model obtained by adding an on-site Hubbard interaction to the Rice–Mele model using infinite time-evolving block decimation, and identified many-body effects in the second-order response function, including a sign reversal of the optical rectification (photovoltaic) response with increasing interaction strength. This also demonstrates that the present framework is practically applicable to advanced methods such as tensor networks.

In a separate study, we revisited terahertz-field-induced second-harmonic generation (TFISH) in ferroelectrics [2]. By deriving time-domain expressions for the polarization modulation $\Delta P$ and the second-harmonic intensity modulation $\Delta I_{\mathrm{SH}}$ induced by a low-frequency pulsed electric field, we clarified how these quantities are governed by nonlinear dynamical susceptibilities. In particular, we showed that $\Delta I_{\mathrm{SH}}$ is not necessarily proportional to $\Delta P$, indicating that the commonly assumed relation $\Delta P \propto \Delta I_{\mathrm{SH}}$ should be used with care when interpreting TFISH measurements.

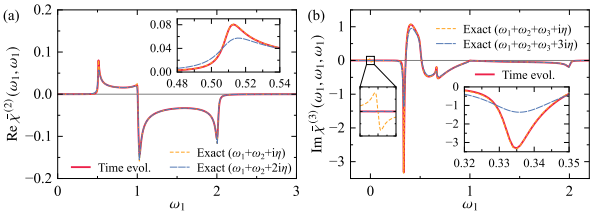


Figure 1: (a) Second- and (b) third-order optical response functions in the Rice–Mele model [1].

## References

[1] A. Ono: Phys. Rev. Lett. **135**, 026401 (2025).

[2] A. Ono: Phys. Rev. B **112**, 115146 (2025).

# Study on the Novel Mechanism of Superconductivity in Nickel Oxides

Hiroshi WATANABE
*Department of Liberal Arts and Basic Sciences, College of Industrial Technology, Nihon University*
*2-11-1 Shin-ei, Narashino, Chiba 275-8576*

The recent discovery of superconductivity in bilayer nickelates [1] has stimulated intensive theoretical efforts to clarify its microscopic pairing mechanism. Although many previous studies have proposed an $s_{\pm}$-type superconducting state, the physical interpretations have often appeared different, because they emphasized different orbitals, bands, or pairing channels. In this project, we addressed this issue by performing large-scale variational Monte Carlo (VMC) calculations for a realistic bilayer nickelate model and clarified the internal structure of the superconducting state [2].

The main purpose of the present study was to determine which superconducting component is primary and which components are induced secondarily by orbital and interlayer hybridization. This distinction is crucial in multiorbital systems, where the optimized gap function may contain several finite components even when only one of them is responsible for the leading pairing instability. We optimized correlated many-body wave functions including superconducting variational parameters and evaluated both the gap structure and equal-time pairing correlations within the same VMC framework.

Our calculations revealed a clear hierarchical structure of superconducting correlations. The primary gap function originates from the bonding–antibonding splitting of the Ni $3d_{z^2}$ orbitals ($\Delta_{zz} \gg \Delta_{xx}$ in Fig. 1), while orbital hybridization redistributes superconducting correlations to the $d_{x^2-y^2}$ channel despite its weak intrinsic pairing interaction. This distinction between the origin of pairing and resulting superconducting correlations explains why the two orbital channels exhibit comparable long-range correlations ($P_{zz} \lesssim P_{xx}$ in Fig. 2). Apparent differences among earlier scenarios can be understood as arising from different representations or projections of the same underlying hierarchical pairing structure.

From the computational point of view, the study required extensive stochastic optimization of many variational parameters and repeated evaluation of correlation functions for large lattice systems, $N = 2\times2\times20\times20 = 1600$ lattice sites in total here. High-performance computing resources were essential for achieving stable convergence, improving statistical accuracy, and systematically exploring the relevant parameter region. The present work demonstrates that large-scale VMC is a powerful method for investigating unconventional superconductivity in strongly correlated multiorbital materials.

In summary, this project established a unified picture of superconductivity in bilayer nickelates by identifying the hierarchical relation between primary and hybridization-induced superconducting correlations. The results resolve an apparent discrepancy among previous theoretical proposals and provide a useful framework for understanding multicomponent superconductivity in correlated layered materials.

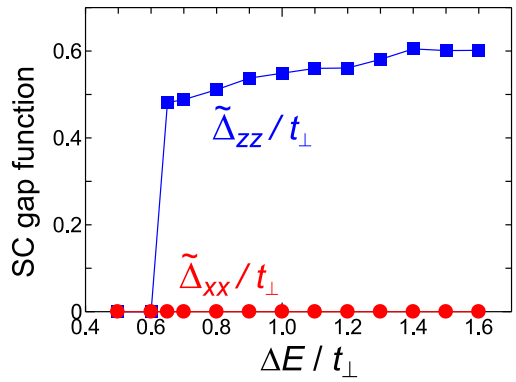


Figure 1: $\Delta E/t_\perp$ dependence of the variational superconducting gap function [2]. $\Delta E$ is a level splitting between $d_{x^2-y^2}$ and $d_{z^2}$ orbitals and $t_\perp$ is an interlayer hopping of the $d_{z^2}$ orbital.

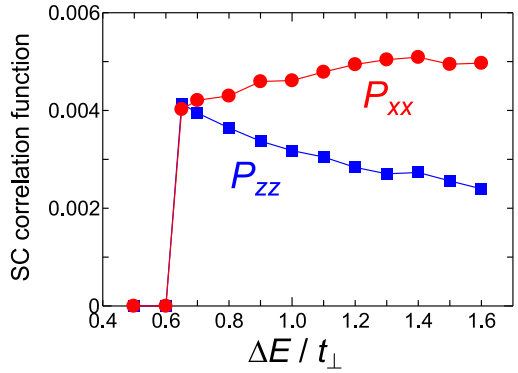


Figure 2: $\Delta E/t_\perp$ dependence of the superconducting correlation function [2].

## References

[1] H. Sun *et al.*, Nature **621**, 493 (2023).

[2] H. Watanabe, H. Sakakibara, and K. Kuroki, arXiv:2603.13604.

# Tensor-train impurity solvers for dynamical mean-field theory

Naoto TSUJI
*Department of Physics, Graduate School of Science, The University of Tokyo*
*Bunkyo, Tokyo 113-0033, Japan*

Strongly correlated electron systems exhibit a wide variety of equilibrium and nonequilibrium phenomena, and dynamical mean-field theory (DMFT) is one of the central theoretical frameworks for their microscopic analysis. In DMFT, a lattice model is mapped onto a quantum impurity model, and the main computational bottleneck lies in solving this impurity problem. In impurity solvers based on perturbative expansions, evaluating higher-order terms requires integration over many internal time variables. As the perturbation order increases, this task becomes a high-dimensional integration problem and quickly becomes computationally demanding. For such problems, the widely used continuous-time quantum Monte Carlo (CT-QMC) method provides a practical approach, but especially for multi-orbital, multi-site, and nonequilibrium impurity models, it suffers from a severe sign problem. In this project, we developed impurity solvers based on tensor-train methods [1, 2] to overcome this difficulty.

To treat these high-dimensional integrals, we employ tensor-train methods, which approximate the integrand in tensor-train format and thereby reduce a multidimensional integration problem to a sequence of one-dimensional integrations. In practice, the tensor-train representation can be constructed using the tensor cross interpolation (TCI) algorithm, which has seen rapid development in recent years. Because this approach is deterministic and does not rely on stochastic sampling, unlike CT-QMC, it is expected to remain effective even for problems in which the sign problem becomes severe in Monte Carlo calculations.

We first combined tensor-train methods with the weak-coupling expansion for equilibrium impurity models [3]. Benchmark calculations for exactly solvable impurity models showed rapid convergence with respect to the tensor-train bond dimension. We then embedded this solver into DMFT for the half-filled Hubbard model on the Bethe lattice and reproduced the metal-to-Mott-insulator transition with an accuracy comparable to that of CT-QMC. An additional advantage of this deterministic tensor-train approach is that the grand potential can also be computed with little extra numerical cost.

We also extended the tensor-train impurity solver to a real-time formulation for nonequilibrium DMFT. Our results show that the integrand of the weak-coupling expansion can be efficiently approximated in tensor-train form even in the real-time formulation. By incorporating this nonequilibrium tensor-train impurity solver into the nonequilibrium DMFT framework, we were able to simulate the dynamics of the Hubbard model after an interaction quench up to times longer than those accessible with CT-QMC in some parameter regimes.

## References

[1] Y. Núñez Fernández *et al.*, Phys. Rev. X **12**, 041018 (2022).

[2] Y. Núñez Fernández *et al.*, SciPost Phys. **18**, 104 (2025).

[3] S. Matsuura *et al.*, Phys. Rev. B **111**, 155150 (2025).

# Spin Inequivalence Enhanced by Coulomb Interaction in a Compensated Ferrimagnet: A 3/4-Filled Inequivalent Dimer Model Study

Akito Kobayashi[a], Kouki Nunota[a], Kazuyoshi Yoshimi[b], Kenichiro Hashimoto[c], and Takahiro Misawa[b]

[a] *Department of Physics, Nagoya University, Nagoya 464-8602*

[b] *Institute for Solid State Physics, University of Tokyo, Kashiwa, Chiba 277-8581, Japan*

[c] *Department of Advanced Materials Science, University of Tokyo, Kashiwa, Chiba 277-8561, Japan*

Collinear antiferromagnets, characterized by antiparallel spin alignment, have traditionally been regarded as incapable of supporting unconventional transport phenomena, such as spin current generation. Recent theoretical developments, however, have identified a class of antiferromagnetic materials—including altermagnets and compensated ferrimagnets—that exhibit unconventional transport properties, notably the anomalous Hall effect and spin current generation. [1, 2, 3].

We previously proposed the possibility of compensated ferrimagnetism in organic compounds with inequivalent dimer structures [4]. We also formulated a simple design principle whereby compensated ferrimagnetism can be realized when antiferromagnetic order emerges in a system comprising two distinct types of dimers. Based on this mechanism, we highlighted the potential realization of compensated ferrimagnetism in the organic compound $(EDO\text{-}TTF\text{-}I)_2ClO_4$ [4].

In this study, we investigate the effects of the on-site Coulomb interaction $U$ in a three-quarter-filled two-dimensional model with inequivalent dimers using mean-field theory. We find that the spin inequivalence in the compensated ferrimagnetic phase is enhanced by $U$. When the bare dimer inequivalence is large, the enhancement due to $U$ outweighs the enhancement of the antiferromagnetic (AF) gap, resulting in the emergence of a band-crossing compensated ferrimagnetic insulator (Fig. 1).

## References

[1] M. Naka et al., Nat. Commun. **10**, 1, (2019)

[2] H. van Leuken et al., Phys. Rev. Lett. **74**, 1171 (1995)

[3] S. Semboshi et al., Sci. Rep. **12**, 10687 (2022)

[4] T. Kawamura et al., Phys. Rev. Lett. **132**, 156502 (2024)

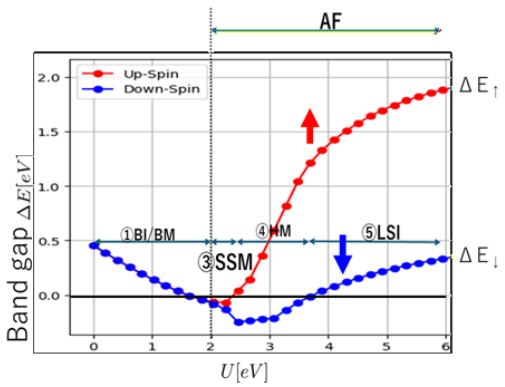


Figure 1: Spin inequivalence enhanced by Coulomb interaction.

# Development of the Fermi Machine and Finite-Temperature Tensor Network Algorithms

Wei-Lin Tu

*Graduate School of Science and Technology,*

*Keio University, Yokohama, Kanagawa 223-8522*

This year, we established a foundational workflow for applying the Fermi Machine wavefunction to quantum many-body systems and achieved notable results, particularly in numerical simulations of the fermionic Hubbard model. The developed method demonstrated high accuracy in ground-state energy calculations, surpassing existing approaches, thereby strongly suggesting that the Fermi Machine could become a new paradigm in quantum many-body research. In particular, extending the previously proposed Fermi Machine framework [1] by introducing a Pfaffian formulation—well suited for representing pairing phases—constitutes a significant advancement. Because the Hubbard model is widely used in studies of high-temperature superconductivity, adopting a Pfaffian wavefunction that naturally captures the pairing structure of the ground state is physically well-motivated and enables a more reliable and expressive description.

Furthermore, strongly correlated systems often exhibit effects that cannot be captured by a wavefunction ansatz alone, making it essential to incorporate neural networks as projection operators. From this perspective, the present study proposed a new convolutional neural network architecture—Tensor-Augmented CNN (TACNN)—that embeds quantum-state structure into the network design [2]. TACNN replaces conventional convolutional kernels with tensors that can be interpreted as small quantum states, and it has already demonstrated significant accuracy improvements in image-classification tasks. By integrating this architecture with the Fermi Machine, we expect to construct a new framework with exceptionally strong expressive power for quantum many-body systems.

Overall, this research opens a new direction for neural quantum states (NQS) and highlights the importance of “AI for Physics” in an era of rapidly advancing AI technologies. We plan to continue enhancing the methodology and expanding its applications in the coming year.

## References

[1] M. Imada, J. Phys. Soc. Jpn. **93**, 104002 (2024).

[2] C.-W. Hsing and W.-L. Tu, arXiv:2604.08072 (2026).

# Electronic Structure Engineering in Low Dimensional Systems with Artificial Nanostructures

Toshikaze KARIYADO

*Research Center for Materials Nanoarchitectonics,*

*National Institute for Materials Science, Namiki, Tsukuba, Ibaraki 305-0044*

We have worked on artificially stacked 2D materials, mainly focusing on moiré systems in which slight mismatches between adjacent layers induce long-range structural patterns. In moiré systems, modelling plays an important role since number of atoms in a moiré unit cell is typically large. When a moiré length is much larger than original lattice spacing, it is possible to define a “local” structure at each position in a moiré unit cell. A widely adopted modelling method is local approximation, where parameters for an effective model are extracted from electronic structure for each “local” structure [1]. This requires large computational resources since the first-principles calculation should be applied to every “local” structure.

$C_{568}$ is a 2D carbon allotrope featured by a square-like lattice structure and co-existence of 5-membered, 6-membered, and 8-membered carbon rings. This allotrope is predicted to be stable in previous numerical studies [2]. Monolayer $C_{568}$ is a semiconductor with its valence top at the M-point in the Brillouin zone, from which we expect interesting tunability of moiré band structures [1,3].

We have successfully built a model for twisted bilayer $C_{568}$ [4] using Quantum Espresso for the first-principles calculations. Using the derived model, it has been also shown that (1) we have a square lattice Hubbard model as an effective model for twisted bilayer C568 at small twist angles, (2) ratio between nearest-neighbor and next-nearest-neighbor transfer integrals depend crucially on the twist angle, and (3) displacement field can induce anisotropy in the nearest-neighbor transfer integrals [4], all of which indicate that twisted bilayer $C_{568}$ serves as an interesting quantum simulator for a square lattice Hubbard model.

## References

[1] T. Kariyado and A. Vishwanath, Phys. Rev. Research **1**, 033076 (2019).

[2] B. Ram and H. Mizuseki, Carbon **158**, 827 (2020).

[3] P. M. Eugenio, Z.-X. Luo, A. Vishwanath, and P. A. Volkov, Phys. Rev. Lett. **134**, 236503 (2025).

[4] T. Kariyado, A. Vishwanath, and Z-X. Luo, Phys. Rev. B 112 125159 (2025).

# Development of computational methods for quantum field theories of nonequilibrium systems utilizing information compression techniques and its applications

Ken INAYOSHI
*Department of Physics, Saitama University*
*255 Shimo-Okubo, Sakura-ku, Saitama City, Saitama 338-8570, Japan*

April 26, 2026

The nonequilibrium Green's function (NEGF) method [1, 2] is a powerful tool for treating many-body correlations and the time evolution of the system on equal footing. However, in nonequilibrium systems, Green's functions depend on two time variables because time-translational invariance is broken. Therefore, long-time simulations incur high memory and computational costs.

To address this challenge, various memory compression techniques have been developed for the NEGF method. Among them, a recent promising approach is the tensor network technique known as the quantics tensor train (QTT) [3]. In prototype implementations of the NEGF method with QTT (the QTT-NEGF method), benchmarks had been limited to the short-time region [4]. To overcome this, in our recent work we implemented a linear-equation solver for the Dyson equation based on a variational approach and demonstrated that nonequilibrium dynamics in large lattice systems can be simulated up to sufficiently long times [5]. However, the cost of this solver grows rapidly with the length of the simulated time domain, making further extension to longer time regions difficult. A key limitation is that this solver does not exploit the causality of Green's functions and globally updates them over the whole time domain within the self-consistent loop. Therefore, it is desirable to incorporate causality into the QTT-NEGF method.

In this project, we developed a causality-based divide-and-conquer method for the QTT-NEGF method [6]. In this method, the self-energy calculation and the self-consistent loop are performed only in the newly added time domain, exploiting the causality of Green's functions. We applied this method to the quench dynamics of the antiferromagnetic state in the Hubbard model using nonequilibrium dynamical mean-field theory. We found that the data size of the stored Green's function is reduced to 1/1000–1/100 of that required by the conventional method [2]. Moreover, the simulation time domain can be extended without a significant increase in the data size.

Further detailed analyses using other physical quantities, such as magnetic response functions, are ongoing on the ISSP Supercomputer.

## References

[1] H. Aoki *et al.*, Rev. Mod. Phys. **86**, 779 (2014).

[2] M. Schüler *et al.*, Comput. Phys. Commun. **257**, 107484 (2020).

[3] H. Shinaoka *et al.*, Phys. Rev. X **13**, 021015 (2023).

[4] M. Murray *et al.*, Phys. Rev. B **109**, 165135 (2024).

[5] M. Środa *et al.*, Phys. Rev. Lett. **135**, 226501 (2025).

[6] K. Inayoshi *et al.*, SciPost Phys. **20**, 077 (2026).